*Progress In Electromagnetics Research B, Vol. 22, 257–283, 2010*

# METHOD OF MODE MATCHING IN TIME DOMAIN

**M. N. Legenkiy and A. Y. Butrym**

Karazin Kharkiv National University
4, Svobody sq., Kharkiv 61077, Ukraine

**Abstract**—A new method is presented for analysis of transient electromagnetic fields in regular structures with abrupt discontinuities. The method is based on mode expansion of the fields in the Time Domain. The modes propagate independently in the regular parts of the structure and are coupled at the discontinuity. The main idea consists in solving 1D FDTD equations for each independent mode channel in the regular waveguides and using mode-matching at the junction cross-section in order to relate the mode amplitudes in all the channels at the same time instant via imposing boundary conditions. As examples the problems of pulse signal diffraction at a step discontinuity in a parallel-plate waveguide, diffraction at a junction of circular and coaxial waveguides, and pulse radiation of a bi-conical antenna are considered. The latter problem is treated as a junction of two conical lines (one of which is the free space) that are regular in spherical coordinates.

## 1. INTRODUCTION

Quite frequently in short pulse electromagnetics one faces problems that can be considered as diffraction at a junction of regular transmission lines. Among such problems we can mention diffraction at step discontinuity in a waveguide, irises, junction of two or more waveguides via some common aperture (see Fig. 1). Even radiation of some antennas as bi-conical, bow-tie, TEM-horn, etc. can be described as diffraction at a junction of two regular conical lines, one of which being the free space, and thus it can be treated within the common framework presented here.

Traditionally in the Frequency Domain (FD) such problems are treated with mode-matching technique that consists in applying Method of Moments to the field continuity boundary conditions written

Corresponding author: M. N. Legenkiy (MLegenkiy@yandex.ru,mlegenkiy@ya.ru).

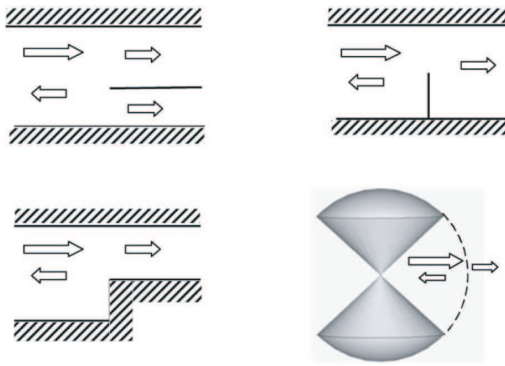

**Figure 1.** Structures that can be modeled by the mode matching method.

in terms of mode expansions of the fields in the regular waveguides being joined. Some useful reviews of Mode Matching Technique in FD can be found, for example, in books [5,,37,,38] and paper [39].

Short pulse signals occupy a wideband spectrum in the FD, which is why FD methods in this case would require calculations at a large number of frequency points and are not appropriate for physical analysis of the waveforms. So such kind of problems is most naturally treated directly in the Time Domain (TD).

There are several numerical techniques available for TD analysis of the problems under consideration. Among them the most popular are the method of Integral Equations in TD (IETD) [1] and Finite Differences in TD (FDTD) [2]. These methods sample surface currents or spatial field distribution and suffer both from numerical problems in achieving high accuracy and from lack of physical insight into the process.

In this paper, we are going to introduce a new calculation method that is based on applying long known in FD methods such as mode expansion [3, 4] and mode matching [5] to the problem being considered in TD.

Transient fields in a regular line can be presented in TD in the form of mode series expansion [6–34] (see detailed description of the publications at the beginning of Section 3 below). Based on such presentation of transient fields in the waveguides we propose an explicit FDTD scheme that consists of 1D FDTD equations for the mode channels and some coupling equation that allows one to update the mode amplitudes at the waveguide junction.

The proposed method reduces errors and computational costs as compared to full-wave FDTD since spatial sampling of the fields is

required only at the junction cross-section and a set of 1D FDTD equations replaces 3D space grid in traditional full-wave FDTD.

The proposed approach has been first presented in conference paper [40, 41]. This contribution is intended to describe more thoroughly the general framework of the method and its implementation details both for cylindrical and conical waveguides along with some illustrative examples.

## 2. FRAMEWORK

In this section, we are going to describe shortly main ideas of the method, show how it relates with mode matching in FD and with full-wave FDTD, and finally give outline of the paper structure.

Among several available FD methods for solving the problem of wave diffraction at abrupt discontinuities in a waveguide the simplest and hence popular is the Mode Matching Technique (MMT) [5]. In this method the structure is considered as a multiport device loaded by characteristic impedances of the corresponding mode channels (see Fig. 2). The field at the discontinuity cross-section is presented in the form of mode series, and then the boundary conditions are imposed in the spatial domain to the sum of the modes. The resulting functional equations are projected onto some testing functions. The testing functions can be chosen to be the same as expansion functions (Ritz-Galerkin method), or some piece-wise interpolating functions (finite elements method), or delta-functions (method of collocations). After applying such a projection one arrives to a System of Linear Algebraic Equations (SLAE) in terms of unknown scattered mode amplitudes.

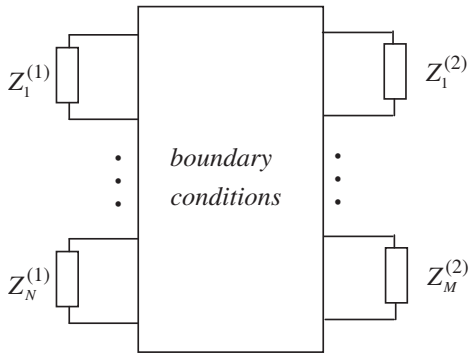


**Figure 2.** A waveguide junction presented as a multiport device loaded by characteristic impedances of the mode channels.

Now let us consider how FDTD method can be applied to solving the waveguide diffraction problem [2]. The structure again is considered as a multiport device. Some spatial domain around the scatterer is sampled over a regular grid points, and the fields in these points are updated in time step-by-step. The incident wave is introduced into the calculation domain via "modal source" typically with Total Field/Scattered Field (TF/SF) technique [2]. The waveguide ports are closed with some Absorbing Boundary Conditions (ABC) (usually UPML [2] is used) that are intended to imitate semi-infinite regular waveguide sections. In some cross-section in the scattered field region near the ABC the wave spatial distribution is projected onto mode functions in order to obtain the waveforms of the reflected and transmitted mode amplitudes. The recorded waveforms can further be subjected to Fourier transform and divided by the incident waveform spectrum in order to obtain frequency spectra of the elements of the S-matrix row that corresponds to the excited modal wave port.

Instead of applying ABC in the spatial domain it was proposed in [45] to use modal matching conditions for launching an incident wave and for separating the scattered fields into the individual mode channels for their further modeling with 1D FDTD. We apply the same approach of using 1D FDTD for the mode channels but we move the FDTD-to-modal interface to the very discontinuity. Actually the spatial domain where the fields should be sampled on some grid is reduced to immediate left and right vicinities of the cross-section that joins the regular waveguides.

So we use 1D FDTD updating formulae for modeling mode channels in the regular parts of the waveguide. The open ends are terminated with effective modal absorbing boundary conditions [36]. In the common cross-section we should sum up the mode functions multiplied by the corresponding mode amplitudes in order to obtain spatial distribution of the field. This distribution should be subjected to Perfect Electric Conductor (PEC) boundary conditions on the flange, the edge singularity condition, and field continuity conditions on the common aperture (or several apertures). Imposing the boundary conditions leads to some equations that should be satisfied for all the spatial points at the flange and the aperture in any time instant. We project these equations on some test functions and obtain a System of Linear Algebraic Equations (SLAE) that relates the mode amplitudes in all the channels on the left and right of the discontinuity. This SLAE being supplemented with the finite difference schemes in each channel results in an explicit formula for updating the mode amplitudes at the discontinuity. The coefficients of the SLAE describe mode coupling,

they don't depend on time and should be calculated only once before starting the time marching.

The procedure that was briefly described above is detailed in the subfollowing sections of the paper. In the third section, we consider mode expansion of the fields, the problem that defines mode functions, and evolutionary equations for the mode amplitudes. The fourth section is devoted to describing a finite difference scheme for solving the evolutionary equations. The procedures of mode channels coupling on the discontinuity, obtaining the coupling matrices, and joining the numerical schemes for different channels are presented in the fifth section of the paper. Some examples of the method implementation are given in the sixth section. The paper ends with conclusions that are formulated in the seventh section. Some mathematical details on derivation of the explicit update FDTD formula are provided as an Appendix to the paper.

## 3. MODE EXPANSION IN TIME DOMAIN

For the first time METD method was proposed by Kisunko in [6] for studying transient fields in homogeneous multi-connected waveguides with Perfect Electric Conductor (PEC) walls. The main idea of the method consists in presenting the sought fields in a waveguide as expansion over independent uncoupled modes with mode amplitudes being governed by some evolutionary equations describing evolution of the waveforms with propagation. Later, Tretyakov has formalized and advanced this approach as Mode Basis Method (MBM) or Evolutionary Approach to Electromagnetics [11–13]. Mode expansion in TD for studying transient fields in different waveguiding structures and cavities has also been used in [14–34].

METD method has been applied to guiding wave problems in several possible geometries by Borisov, namely for cylindrical, conical, and sectorial waveguides [7–10]. A similar technique for spherical coordinate system in the free space, radial inhomogeneous medium, and conical lines has been used later by Shlivinski and Heyman [31]. MBM in spherical coordinate system for angular inhomogeneous conical structures was considered in [34].

We are going to consider METD in cylindrical and spherical coordinates. The former allows consideration of any closed cylindrical waveguide (rectangular, circular, coaxial, parallel-plate, etc.), while the latter allows analysis of conical line structures including free space, biconical lines, cones, planar cones (bow-tie antennas), TEM-horns, and similar structures that are widely used as ultrawideband antennas.

### 3.1. METD in Cylindrical Coordinates

Mode Basis Method is based on presenting sought fields in the form of mode series with mode amplitudes being functions of longitudinal coordinate and time [12]. For example modal series for TM-waves can be written as [19]

$$\begin{aligned}\varepsilon_0^{1/2}\vec{E}\left(\vec{r}_\perp,z,t\right)&=\textstyle\sum_n\left[V_n\left(z,t\right)\nabla_\perp\varphi_n\left(\vec{r}_\perp\right)+\vec{z}_0 e_n\left(z,t\right)\kappa_n^2\varphi_n\left(\vec{r}_\perp\right)\right],\\ \mu_0^{1/2}\vec{H}\left(\vec{r}_\perp,z,t\right)&=\textstyle\sum_n I_n\left(z,t\right)\left[\vec{z}_0\times\nabla_\perp\varphi_n\left(\vec{r}_\perp\right)\right]\end{aligned} \tag{1}$$

Here $\varphi_n\left(\vec{r}_\perp\right)$ are scalar potentials that define mode configurations. They can be found as solutions to the following Dirichlet boundary eigenvalue problem [12]:

$$\left(\nabla_\perp^2+\kappa_n^2\right)\varphi_n(\vec{r}_\perp)=0;\quad \varphi|_L=0 \tag{2}$$

$\kappa_n$ are the eigenvalues that determine cutoff frequencies for a hollow waveguide; $n$ is the mode index. A similar presentation can be written for TE-waves with scalar mode functions satisfying a similar Neumann problem.

The mode amplitudes in the expansion (1) are governed by the following System of Evolutionary Equations (SEE) [12, 20]

$$\begin{cases} e_n\kappa_n^2=\partial_\tau I_n+\partial_z V_n,\\ I_n=-\partial_\tau e_n,\\ \partial_z I_n=-\partial_\tau V_n\end{cases} \tag{3}$$

here $\tau=ct$, $\partial_\tau=c^{-1}\partial/\partial t=\sqrt{\varepsilon_0\varepsilon\mu_0}\partial_t$, $c=c_0/\sqrt{\varepsilon}$ is the speed of light in the medium. This system can be reduced to a single Klein-Gordon equation (KGE) for each mode:

$$\left(\partial_\tau^2-\partial_z^2+\kappa^2\right)I=0 \tag{4}$$

This equation describes propagation of an arbitrary wave in a regular uniformly filled waveguide. Analytical solution to this equation is known in the form of convolution of initial-boundary condition with a transport operator expressed in terms of Bessel functions [19, 35].

### 3.2. METD in Spherical Coordinates

A similar approach formulated in spherical coordinate system can be applied for description of electromagnetic fields in conical lines and free space [21, 34]. In further derivation for brevity sake we will only consider TEM- and TM-waves as an example; TE-waves can be considered similarly.

The full fields in spherical coordinate system can be written in angular-radial form as follows:

$$\begin{array}{c} \vec{\mathcal{E}}(\vec{r},t) = \vec{E}(\vec{r},t) + \vec{r}_0 E_r(\vec{r},t) \\ \vec{\mathcal{H}}(\vec{r},t) = \vec{H}(\vec{r},t) \end{array} \tag{5}$$

where $\vec{r}_0$ is the unit radial ort, $\vec{r} = \{r, \theta, \varphi\}$ are coordinates in the spherical coordinate system, $t$ is the time coordinate, $\vec{E}$ and $\vec{H}$ are the angular field components ($\theta$ and $\varphi$ components).

The angular and radial components of the sought fields can be presented in the form of mode series as follows [31, 34, 41]:

$$\begin{array}{l} \sqrt{\varepsilon_0}\vec{E}(r,\theta,\varphi,t) = \frac{1}{r}\left\{\sum\limits_n V_n(r,t)\,\vec{E}_n(\theta,\varphi) + \sum\limits_k V_k^T(r,t)\,\vec{E}_k^T(\theta,\varphi)\right\} \\ \sqrt{\mu_0}\vec{H}(r,\theta,\varphi,t) = \frac{1}{r}\left\{\sum\limits_n I_n(r,t)\,\vec{H}_n(\theta,\varphi) + \sum\limits_k I_k^T(r,t)\,\vec{H}_k^T(\theta,\varphi)\right\} \\ \sqrt{\varepsilon_0}E_r(r,\theta,\varphi,t) = \frac{1}{r^2}\sum\limits_n e_n(r,t)\,q_n\varphi_n(\theta,\varphi) \end{array} \tag{6}$$

The scalar and vector functions dependent on angular variables are the basis functions of the expansion; they constitute the so-called mode basis. The expansion coefficients that are scalar functions dependent only on the radial and time variable are called as mode amplitudes. The quantities with superscript T describe TEM-waves. There can be only finite number of TEM-waves that depends on connectivity of the PEC cones. There are no TEM-waves in the expansion of fields in the free space.

Scalar basis functions for TM-modes in a conical line can be obtained from the following eigenvalue problem with Dirichlet boundary conditions at the cones:

$$\begin{cases} \nabla_\perp \cdot \nabla_\perp \Phi_n + q_n^2 \Phi_n = 0 \\ \Phi_n|_L = 0 \end{cases} \tag{7}$$

where $q_n$ are the eigenvalues; $\Phi_n$ are the eigenfunctions; $\nabla_\perp = \vec{\theta}_0\,\partial/\partial\theta + \vec{\varphi}_0\,(1/\sin\theta)\,\partial/\partial\varphi$ is the angular part of Hamilton $\nabla$ operator, $L$ is the contour of the PEC cones.

Vector basis functions of the conical line can be expressed via the scalar basis functions as follows:

$$\vec{E}_n = q_n^{-1}\nabla_\perp \Phi_n \quad \vec{H}_n = q_n^{-1}\left[\vec{r}_0 \times \nabla_\perp \Phi_n\right] \tag{8}$$

Scalar basis functions for TEM-mode in the conical line are determined from the following inhomogeneous boundary problem:

$$\begin{cases} \nabla_\perp \cdot \nabla_\perp \Phi^T = 0 \\ \Phi^T\big|_{L_j} = d_j \end{cases} \tag{9}$$

where $d_j$ are some constants on the $j$-th part of the multi-connected contour $L$.

Vector basis function of the TEM-wave can be expressed via the scalar basis function as follows:

$$\vec{E}^T = \nabla_\perp \Phi^T \quad \vec{H}^T = \left[\vec{r}_0 \times \nabla_\perp \Phi^T\right] \tag{10}$$

By solving problem (7), (9) and applying formulae (8), (10) a mode basis can be constructed in any conical line (in the free space as well)

Substitution of field expansion (6) into Maxwell equations yields the following system of radial evolutionary equations for the mode amplitudes [34, 41]

$$\begin{cases} \partial_\tau I_n(r,t) + \partial_r V_n(r,t) - \left(\frac{q_n}{r}\right)^2 e_n(r,t) = 0, \\ \partial_\tau e_n(r,t) + I_n(r,t) = 0, \\ \partial_\tau V_n(r,t) + \partial_r I_n(r,t) = 0. \end{cases} \tag{11}$$

This system holds for TM-waves in a conical line and in the free space. For a TEM-wave in a conical line the governing equation can be reduced to

$$\begin{cases} \partial_\tau I_k^T(r,t) + \partial_r V_k^T(r,t) = 0, \\ \partial_\tau V_k^T(r,t) + \partial_r I_k^T(r,t) = 0 \end{cases} \tag{12}$$

From (11) one can derive the following 2-nd order equation known as Klein-Gordon-Fock equation (KGFE) [31, 34]:

$$\left[\partial_\tau^2 - \partial_r^2 + (q_n/r)^2\right] e_n(r,t) = 0 \tag{13}$$

Analytical solution to the Klein-Gordon-Fock equation exists only for free space when $q_n^2 = n(n+1)$ [21, 31].

System (12) yields the wave equation:

$$\left[\partial_\tau^2 - \partial_r^2\right] V_k^T(r,t) = 0 \tag{14}$$

## 4. NUMERICAL SOLUTION OF THE SYSTEM OF EVOLUTIONARY EQUATIONS

The obtained evolutionary equations (3) and (11) should be supplemented with initial and/or initial-boundary conditions. The resulted problem is solved numerically using finite-difference method.

### 4.1. Numerical Solution of the Waveguide Evolutionary Equations

Using finite-difference approximation to the derivatives in (3) it is easy to obtain the following explicit update formulae (details can be found in [19, 35]):

$$\begin{cases} I|_i^{k+1/2} = I|_i^{k-1/2} + \kappa^2 \Delta\tau \; e|_i^k - \frac{\Delta\tau}{\Delta z}\left(V|_{i+1/2}^k - V|_{i-1/2}^k\right), \\ e|_i^{k+1} = e|_i^k - \Delta\tau \; I|_i^{k+1/2}, \\ V|_{i+1/2}^{k+1} = V|_{i+1/2}^k - \frac{\Delta\tau}{\Delta z}\left(I|_{i+1}^{k+1/2} - I|_i^{k+1/2}\right), \end{cases} \tag{15}$$

The time-space grid and the stencils of these equations are sketched in Fig. 3.

Solution of these finite-difference equations yields approximation to the solution of the original SEE. It converges quadratically to the exact one with error decreasing as $C_1(\Delta\tau)^{-2} + C_2(\Delta z)^{-2}$.

It is known that for the wave equation a solution of the finite-difference equation can yield an exact solution when $\Delta\tau, \Delta z$ are chosen properly (at the stability limit) [2]. In such case the dispersion relation of the finite-difference equation coincides with that of the original differential equation. A similar situation holds for KGE, though the dispersion relations don't equal exactly but the discrepancy grows not as $\omega^{3.5}$ but as $\omega^1$ (for $\omega \gg c\kappa$) when $\Delta\tau, \Delta z$ are chosen at the stability limit, which for KGE is [35]:

$$\Delta\tau \leq \frac{2\Delta z}{\sqrt{\kappa^2 \Delta z^2 + 4}} \tag{16}$$

For larger time steps the update equations (15) result in unstable (increasing) solution. By choosing $\Delta z$ slightly greater than the stability limit (16) it is possible to adjust the numerical dispersion error to be

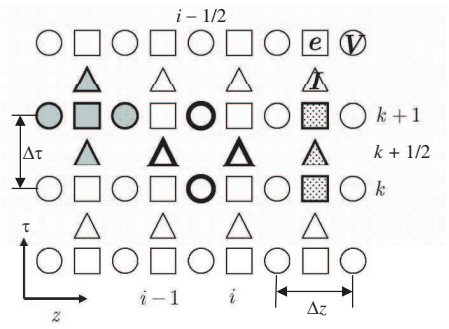


**Figure 3.** Finite-difference stencils used in the SEE.

minimal in some frequency range. We exploit this property in the further analysis by choosing different $\Delta z$ in each of the coupled mode channels while $\Delta\tau$ being common in order to avoid time interpolation while matching.

### 4.2. Numerical Solution of the Radial Evolutionary Equations

Numerical solution of the radial evolutionary equations is not widely known so we describe it in more details. It is important to notice that since the cutoff frequency of a spherical mode depends on the radial coordinate ($\omega_c(r) = q_n^2/r^2$) [21] FDTD solution of the SEE with uniform radial step for the conical line can result in large computational errors at small $r$. So we need to vary radial steps with radius. The radial step for each mode channel is chosen from two conditions. First, at any radius the mode cut-off wavelength has to be sampled sufficiently densely (we use 40 points per the cut-off wavelength in the simulation). Second, the smallest wavelength of interest in the excitation signal has to be sufficiently sampled. Based on these conditions a non-uniform radial grid for the mode amplitude of the transverse electric field component ($V$ in (11)) is chosen. For convenience the nodes for the others mode amplitudes ($e$ and $I$) are placed in the middle between the nodes for $V$. As a result a grid for $e$ and $I$ also has non-uniform radial steps.

Using non-uniform steps is important for the centre vicinity where the cut-off frequency becomes large enough at some radius so that any constant-size step becomes too coarse compared with the cut-off wavelength. Another consequence of this growth of the cut-off frequency is that any wave becomes evanescent at some small radius so absorbing boundary conditions can be specifically designed assuming evanescent regime or can be considered needless because of natural decay of the evanescent waves. From the other hand the radial step at large radius cannot grow constantly because of requirement of fine sampling the smallest wavelength of interest in the excitation signal. So it is convenient to choose a constant step starting from some radius.

In particular, considering a problem of wave radiation into free space by a finite length conical-line antenna, the radial step at the end of the conical line in each mode channel is chosen to be sufficiently small so that there is at least 40 points per minimum wavelength of interest (cut-off wavelength or minimal wavelength in the excitation signal spectrum whichever is smaller). Then the inner region mode channels (antenna region) use non-uniform radial steps decreasing as $\Delta r \sim r$ while the outer region (free space) mode channels use constant radial step.

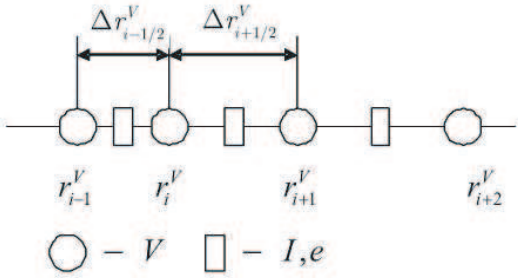


**Figure 4.** Non-regular radial step.

Time sampling of the mode amplitudes in (11) is based on the widely known "leap-frog" scheme [2]. The mode amplitudes of the electric fields ($e$ and $V$) are calculated at time instants $k\Delta\tau$ and the mode amplitude of the magnetic field $I$ is evaluated at $(k + 1/2)\Delta\tau$. Time step should be common to all the mode channels, it is defined by the smallest $\Delta r$ used in calculations and is chosen based on stability criterion. In order to derive finite difference expressions for the SEE in the case of varying radial step we integrate the evolutionary equation over the finite segments.

For the first equation in (11) the integration interval is from $r^V_i$ to $r^V_{i+1}$ (see Fig. 4). In order to obtain a second order accurate scheme $e$ and $I$ mode amplitudes are assumed to be constant within the integration interval. Integrating $\partial_r V$ and $q^2 e/r^2$ and using central finite difference for approximation of time derivative we have derived the following update formula

$$\partial_\tau I + \partial_r V - q^2 e/r^2 = 0$$

$$\Rightarrow I|^{k+1/2}_{i+1/2} = I|^{k-1/2}_{i+1/2} + \frac{q^2\Delta\tau}{r^V_i\, r^V_{i+1}}\, e|^k_{i+0.5} - \frac{\Delta\tau}{\Delta r^V_{i+1/2}}\left(V|^k_{i+1} - V|^k_i\right) \quad (17)$$

where $\Delta r^V_{i+1/2} = r^V_{i+1} - r^V_i$.

The second equation in (11) does not depend on the spatial coordinate and is easily approximated by the time finite difference:

$$\partial_\tau e = -I \Rightarrow e|^{k+1}_{i+1/2} = e|^k_{i+1/2} - \Delta\tau\ I|^{k+1/2}_{i+1/2} \quad (18)$$

In the third equation in (11) the integration is performed from $\left(r^V_{i-1} + r^V_i\right)/2$ to $\left(r^V_i + r^V_{i+1}\right)/2$. As a result we have derived the

following updating formula

$$\partial_\tau V = -\partial_r I \;\Rightarrow V|_i^{k+1} = V|_i^k - \frac{2\Delta\tau}{\Delta r^V_{i+1/2} + \Delta r^V_{i-1/2}} \left( I|_{i+1/2}^{k+1/2} - I|_{i-1/2}^{k+1/2} \right) \tag{19}$$

Gathering all together, the explicit update formulae for marching on time can be written as:

$$\begin{cases} I|_{i+1/2}^{k+1/2} = I|_{i+1/2}^{k-1/2} + \frac{q^2\Delta\tau}{r_i^V r_{i+1}^V}\, e|_{i+1/2}^k - \frac{\Delta\tau}{\Delta r^V_{i+1/2}} \left( V|_{i+1}^k - V|_i^k \right) \\ e|_{i+1/2}^{k+1} = e|_{i+1/2}^k - \Delta\tau\; I|_{i+1/2}^{k+1/2} \\ V|_i^{k+1} = V|_i^k - \frac{2\Delta\tau}{\Delta r^V_{i+1/2} + \Delta r^V_{i-1/2}} \left( I|_{i+1/2}^{k+1/2} - I|_{i-1/2}^{k+1/2} \right) \end{cases} \tag{20}$$

In order to solve the SEE efficiently one needs some absorbing boundary conditions bounding the finite simulation domain. For the coordinate centre vicinity we can do without any absorbing condition since each mode becomes evanescent at any given frequency when the radial coordinate becomes less than some radius. The absorbing boundary condition for the TEM-wave can be easily derived as impedance boundary condition since there is no dispersion in this channel. The channels in the free space region can be efficiently bounded by the 'exact' absorbing boundary condition proposed by Sirenko in [46].

## 5. MODE MATCHING IN NUMERICAL SIMULATION

The modes can be calculated independently everywhere except for the waveguide junction point. At this point we should apply boundary conditions at the aperture and the flange in order to relate all the mode amplitudes on the left and right from the junction.

In further consideration, in order to speak more specifically, we consider a junction like a waveguide step where there are two waveguides: a narrow one and a wide one, which are coupled via aperture that occupies the whole cross-section of the narrow waveguide (see an example of such a structure on the inset in Fig. 5).

In order to derive update formulae for matching the mode amplitudes we are going to use the equation for time derivative of electric mode amplitude that looks similarly for cylindrical (see 3rd of Eq. (3)) and spherical (see 3rd of Eq. (11)) coordinate systems

$$\begin{array}{ll} \partial_\tau V = -\partial_r I & \text{for conical waveguide} \\ \partial_\tau V = -\partial_z I & \text{for cylindrical waveguide} \end{array} \tag{21}$$

So the following derivation will be valid for both cases with the only difference in changing notation for propagation coordinate $r \leftrightarrow z$.

It is known that if the numerical boundary conditions have one order less accurate than the interior accuracy, then the order of the global accuracy is preserved [48]. That's why at the boundary we will use left finite differences instead of the central one used in (15) and (20). It yields the following update formula for each mode channel:

$$V^{(n)}\Big|_0^{k+1} = V^{(n)}\Big|_0^{k} - \frac{2\Delta\tau}{\Delta r_{-1/2}^{(n)}}\left(I^{(n)}\Big|_0^{k+1/2} - I^{(n)}\Big|_{-1/2}^{k+1/2}\right) \tag{22}$$

The spatial index $|_0$ corresponds to the junction position. At that $I^{(n)}|_{-1/2}^{k+1/2}$ denotes magnetic field mode amplitude in the left mode channel $\#n$ at distance $\Delta r_{-1/2}^{(n)}/2$ before the junction; $\Delta r_{-1/2}^{(n)}$ is the radial step before the discontinuity (it can be different for each mode channel and is varied for conical lines as described in Section 4.2).

The update formula (22) can be written for all the channels simultaneously using matrix notation:

$$\begin{aligned} &\mathbf{v}^{(1)}|_0^{k+1} = \mathbf{v}^{(1)}|_0^{k} - 2\mathbf{S}^{(1)} \cdot \left(\mathbf{i}^{(1)}|_0^{k+1/2} - \mathbf{i}^{(1)}|_{-1/2}^{k+1/2}\right) \\ &\mathbf{S}^{(1)} = \mathrm{diag}\left(\Delta\tau/\Delta r_{-1/2}^{(n)}\right) \end{aligned} \tag{23}$$

here small bold values $\mathbf{v}^{(1)}$ and $\mathbf{i}^{(1)}$ are the vectors of the corresponding mode amplitudes for all the channels in the waveguide #1 (the narrow one), and $\mathbf{S}^{(1)}$ is the diagonal matrix of Courant-Friedrichs-Lewy numbers $S = \Delta\tau/\Delta r$ in the mode channels [1]. Similarly to (23) one can write for the wide waveguide (#2) the following update formula using right finite difference:

$$\begin{aligned} &\mathbf{v}^{(2)}|_0^{k+1} = \mathbf{v}^{(2)}|_0^{k} - 2\mathbf{S}^{(2)} \cdot \left(\mathbf{i}^{(2)}|_{1/2}^{k+1/2} - \mathbf{i}^{(2)}|_0^{k+1/2}\right) \\ &\mathbf{S}^{(2)} = \mathrm{diag}\left(\Delta\tau/\Delta r_{+1/2}^{(n)}\right) \end{aligned} \tag{24}$$

The boundary conditions require continuity of tangential field components at the common aperture and zero tangential electric field at the flange:

$$\begin{aligned} &\sum_m \left(\mathbf{v}^{(1)}|_0^k\right)_m \vec{E}_m^{(1)}(\vec{r}_\perp) = \begin{cases} \sum\limits_{m'} \left(\mathbf{v}^{(2)}|_0^k\right)_{m'} \vec{E}_{m'}^{(2)}(\vec{r}_\perp), & \vec{r}_\perp \in \text{Aperture} \\ 0, & \vec{r}_\perp \in \text{Flange} \end{cases} \\ &\sum_m \left(\mathbf{i}^{(1)}|_0^k\right)_m \vec{H}_m^{(1)}(\vec{r}_\perp) = \sum_{m'} \left(\mathbf{i}^{(2)}|_0^k\right)_{m'} \vec{H}_{m'}^{(2)}(\vec{r}_\perp), \quad \vec{r}_\perp \in \text{Aperture} \end{aligned} \tag{25}$$

We apply Method of Moments procedure in order to reduce these functional equations to a set of linear algebraic equations for the moments. As testing functions for field projection we use the basis

of mode functions of the wide waveguide #2 in the first continuity condition (25), and the basis of the narrow waveguide #1 — in the second continuity condition. It yields the matrix formulation of the boundary conditions as

$$\begin{cases} \mathbf{M} \cdot \mathbf{v}^{(1)}|_0^k = \mathbf{v}^{(2)}|_0^k \\ \mathbf{i}^{(1)}|_0^{k+1/2} = \mathbf{M}^T \cdot \mathbf{i}^{(2)}|_0^{k+1/2} \end{cases} \tag{26}$$

where $T$ denotes transposition, and the transform matrix $\mathbf{M}$ is defined as follows:

$$M_{mm'} = \int \vec{E}_m^{(1)}(\vec{r}_\perp) \cdot \vec{E}_{m'}^{(2)}(\vec{r}_\perp)\, dS \tag{27}$$

Using formulae (23), (24), and (26) the following update equations for the electric field modal amplitudes at the junction can be derived (see Appendix A for details):

$$\begin{aligned} \mathbf{v}^{(1)}|_0^{k+1} &= \mathbf{v}^{(1)}|_0^k + 2\mathbf{F}^{-1} \cdot \left( \mathbf{i}^{(1)}|_{-1/2}^{k+1/2} - \mathbf{M}^T \cdot \mathbf{i}^{(2)}|_{1/2}^{k+1/2} \right), \\ \mathbf{v}^{(2)}|_0^{k+1} &= \mathbf{M} \cdot \mathbf{v}^{(1)}|_0^{k+1}. \end{aligned} \tag{28}$$

where matrix $\mathbf{F}$ has been introduced as follows:

$$\mathbf{F} = \left( \mathbf{S}^{(1)} \right)^{-1} + \mathbf{M}^T \cdot \left( \mathbf{S}^{(2)} \right)^{-1} \mathbf{M} \tag{29}$$

## 6. NUMERICAL RESULTS

### 6.1. Step in a Parallel-plate Waveguide

The first structure that we are going to analyze is a step discontinuity in a parallel-plate waveguide. Diffraction of a TEM-wave launched in a wide waveguide ($a = 1$) towards a junction with a narrow waveguide ($b = 0.6$) is considered (see inset in Fig. 5). The problem was solved by the proposed method and results were compared against the exact solution obtained by MMT in FD [5]. The mode functions in this case are expressed via trigonometric functions [3], and the corresponding coupling matrix (27) can be easily obtained in a closed-form.

We take into consideration TEM-mode in the wide and narrow sections and additionally 8 TM-modes in the wide waveguide and 5 TM-modes in the narrow one in accordance with Mittra rule [5], which requires that the transverse wavenumbers of the highest considered modes in the matched waveguides are approximately equal. Excitation pulse has Gaussian waveform (see Fig. 5) with parameters $T = 0.4\, a/c_0$, $t_0 = 3$ T.

In the FDTD modeling the time step was chosen so that the maximal cut-off frequency for all the considered modes was sampled

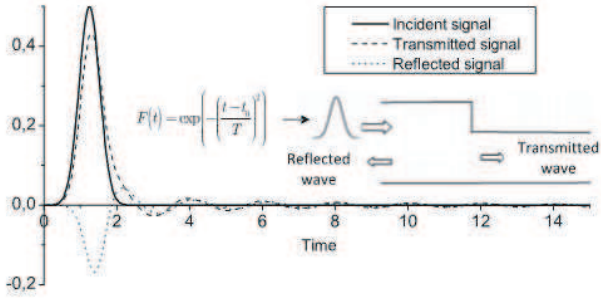


**Figure 5.** The waveforms of the incident and diffracted TEM-modes.

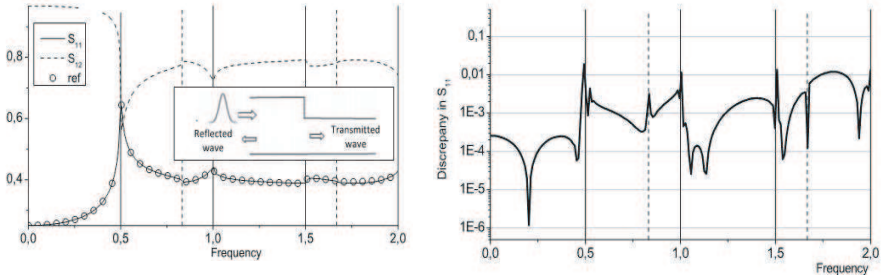


**Figure 6.** Transmission and reflection coefficients.

with at least 8 points per period. In this simulation $\Delta t = 0.03$. The spatial steps $\Delta z$ for each mode are chosen individually at the limit of stability criterion (16). We performed 4096 time steps in the modeling. The resulted waveforms of the incident, reflected, and transmitted TEM-modes are shown in Fig. 5.

In Fig. 6 the calculated spectra of the reflection and transmission coefficients for TEM-modes are presented. The solid (dashed) vertical lines in the picture mark the cut-off frequencies for the wide (narrow) waveguide. The calculated data match well with the reference results obtained by FD MMT [5]. The discrepancy grows with frequency (due to quadratic order of approximation of FDTD-scheme) and has spikes at the cut-off frequencies due to spectrum discontinuities at these points.

### 6.2. Junction of Coaxial and Circular Waveguides

Next we consider a junction of coaxial and circular waveguides (see geometry on the inset in Fig. 7). The outer radius is $b = 0.5$, the inner radius is $a = 0.1$.

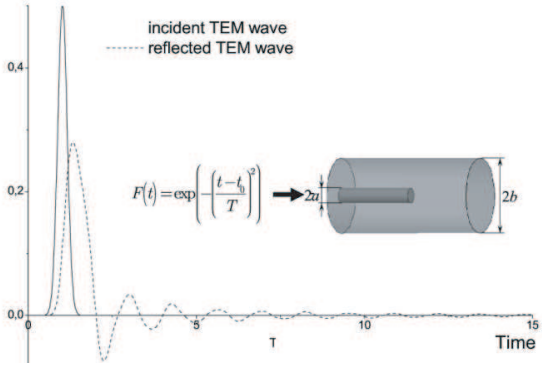


**Figure 7.** TEM-mode waveforms.

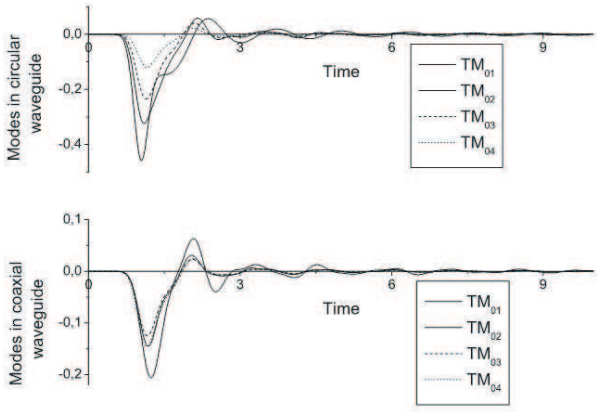


**Figure 8.** Waveforms of transmitted (top) and reflected (bottom) TM-modes.

Mode functions for the coaxial and circular waveguides are well known [4], the coupling matrix elements are easily calculated as integrals from Bessel functions. In the circular waveguide we took into account 5 TM-modes. In the coaxial waveguide we considered TEM-mode and 4 TM-modes in accordance with Mittra rule [5].

The TEM-wave is launched in the coaxial waveguide towards the junction. The excited waveform has Gaussian form (see Fig. 7) with parameters $T = 0.2\,a/c_0$, $t_0 = 5$ T. The time step was chosen similarly to the previous case but with 15 points per smallest cut-off wavelength, it yields $\Delta t = 0.013$. Spatial steps $\Delta z$ were chosen for each mode at the stability limit. 4096 time steps were performed in the modeling. The

resulting waveforms are depicted in Figs. 7–8. Fig. 9 shows comparison of the calculated reflectivity spectrum for TEM-mode with the results obtained by a commercial solver. Solid/dash lines in the graph mark the cut-off frequencies of the circular/coax waveguides correspondingly.

### 6.3. Bi-conical Antenna

Now we are going to consider some radiation problem. A bi-conical antenna shown in Fig. 10 is widely used for radiating ultrawideband short pulses. It is the simplest multi-cone like line that supports propagation of TEM-mode. We chose it for consideration since its mode functions can be obtained in a closed-form.

The antenna is excited with a TEM-wave that diffracts into TM-waves at the open end (antenna aperture), at this TE-waves are not excited and there is no radial magnetic field component due to symmetry.

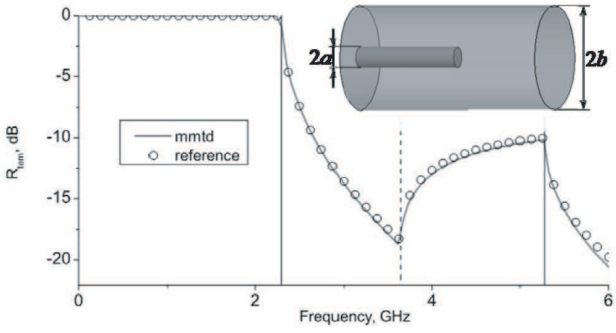


**Figure 9.** $S_{11}$ for TEM-wave.

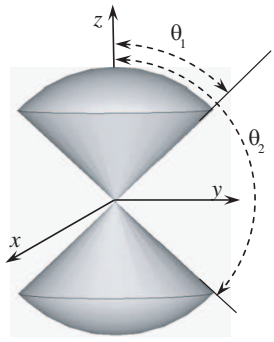


**Figure 10.** Bi-conical antenna.

*6.3.1. Basis in the Bi-cone Region*

The solution to the boundary problem (7) for a nonsymmetrical bi-cone (Fig. 10) can be presented via Legendre functions of first kind $P_{\mu_n}(\ )$ as follows [21, 34, 49]:

$$\Phi_n^{TM}(\theta) = C_n \left[ P_{\mu_n}(\cos(\theta)) - \frac{P_{\mu_n}(\cos(\theta_1))\, P_{\mu_n}(-\cos(\theta))}{P_{\mu_n}(-\cos(\theta_1))} \right] \tag{30}$$

where $\mu_n$ are defined from the following dispersion relation:

$$\begin{vmatrix} P_{\mu_n}(\cos(\theta))|_{\theta=\theta_1} & P_{\mu_n}(-\cos(\theta))|_{\theta=\theta_1} \\ P_{\mu_n}(\cos(\theta))|_{\theta=\theta_2} & P_{\mu_n}(-\cos(\theta))|_{\theta=\theta_2} \end{vmatrix} = 0 \qquad \begin{matrix} \mu_n \neq 0, \pm 1, \pm 2, \ldots \quad \theta \in [\theta_1, \theta_2] \quad n \in \mathrm{N} \end{matrix} \tag{31}$$

Eigenvalues $q_n$ of the problem (7) can be expressed via $\mu_n$ as follows:

$$q_n^2 = \mu_n(\mu_n + 1) \tag{32}$$

The normalization constants $C_n$ in (30) are defined by the condition:

$$\frac{1}{4\pi} \int\limits_{\Omega} \Phi_n^{TM}(\theta) \Phi_{n'}^{TM}(\theta) d\Omega = \delta_{nn'} \tag{33}$$

The corresponding vector basis functions can be found using (8) as:

$$\vec{E}_n^{TM}(\theta) = \vec{\theta}_0 q_n^{-1} \partial \Phi_n^{TM} / \partial \theta, \quad \vec{H}_n^{TM}(\theta) = \vec{\varphi}_0 q_n^{-1} \partial \Phi_n^{TM} / \partial \theta \tag{34}$$

TEM-mode can be obtained as a solution to the boundary problem (9) that yields:

$$\Phi^T(\theta) = C \ln \frac{1 - \cos\theta}{\sin\theta} \tag{35}$$

$$\vec{E}^T(\theta) = \vec{\theta}_0 \frac{C}{\sin\theta}, \quad \vec{H}^T(\theta) = \vec{\varphi}_0 \frac{C}{\sin\theta} \tag{36}$$

where normalization constant $C$ is determined from the condition:

$$\frac{1}{4\pi} \int\limits_{\Omega} \left[ \vec{E}^T(\theta) \right]^2 d\Omega = 1 \tag{37}$$

*6.3.2. Basis in the Free Space*

In order to build a mode basis for TM-waves in the free space one should solve the eigenvalue problem (7) assuming finiteness and periodicity boundary conditions on the unit sphere. The solution

to this problem is well known and has the following form (spherical harmonics) [31]:

$$\begin{aligned} &\Phi_n^{TM}(\theta) = \sqrt{2n+1}\, P_n\left(\cos(\theta)\right) \\ &q_n^2 = n(n+1), \;\; n \in \mathbb{N}, \;\; \theta \in [0, \pi] \end{aligned} \tag{38}$$

The corresponding vector basis functions are:

$$\begin{aligned} \vec{E}_n^{TM}(\theta) &= \frac{\vec{\theta}_0}{\sin\theta}\sqrt{\frac{n(n+1)}{2n+1}}\left[P_{n+1}\left(\cos(\theta)\right) - P_{n-1}\left(\cos(\theta)\right)\right] \\ \vec{H}_n^{TM}(\theta) &= \frac{\vec{\varphi}_0}{\sin\theta}\sqrt{\frac{n(n+1)}{2n+1}}\left[P_{n+1}\left(\cos(\theta)\right) - P_{n-1}\left(\cos(\theta)\right)\right] \end{aligned} \tag{39}$$

For numerical simulation we consider a symmetric bi-conical antenna with radius $R = 10\,\text{mm}$ and the cone angle $\theta_1 = 46,98°$. Such a bi-conical line has wave impedance $100\,\Omega$ [47]. The antenna is fed at apex by a Gaussian pulse with parameters $T = 50\,\text{ps}$ and $t_0 = 5\,\text{T}$ (see Fig. 11) that launches a TEM-wave propagating from centre to the open end of the antenna.

In the free space we take into account 20 TM-modes in order to describe properly all the harmonics that can be exited by the used pulse at antenna end. In the bi-conical line we considered the TEM-mode and 9 TM-modes in accordance with Mittra rule [5].

The spatial grid in the conical line is nonuniform, the radial step size is chosen as described in Section 4.2. The time step was chosen from the stability criterion for the minimal used radial step. 4096 time steps were performed. The calculated return loss is plotted in time and frequency domains in Fig. 11. The data are compared against the results obtained by a commercial 3D FDTD solver. There is a small discrepancy at early time that is caused by errors in modeling vicinity of the feeding point in 3D FDTD, while at the later time agreement is near perfect. The discrepancy in the frequency domain is caused by the above mentioned reflection at the feed point in the FDTD.

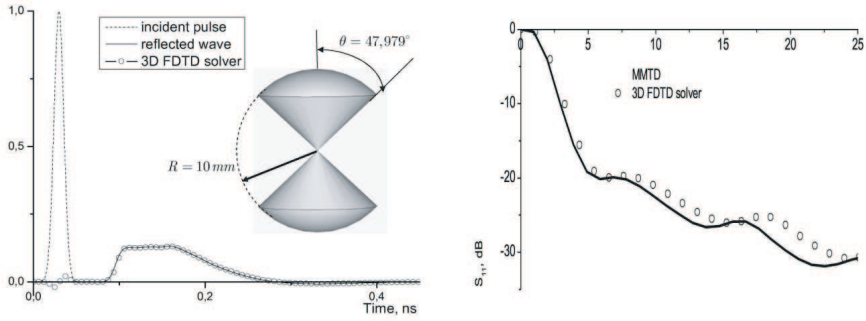


**Figure 11.** Return loss in the bi-cone antenna.

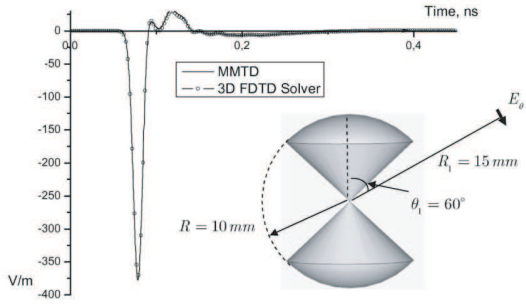


**Figure 12.** Waveforms calculated in the near zone.

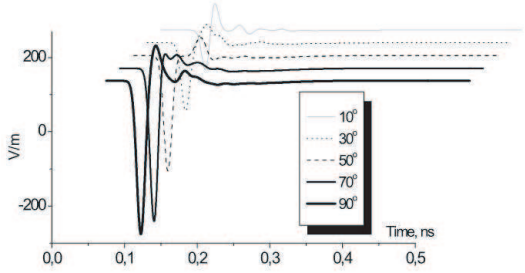


**Figure 13.** Near field waveforms.

The waveforms of the radiated spherical harmonics in the free space were obtained in MMTD modeling at radius $R_1 = 15\,\text{mm}$. Then they were summed up with the angle dependencies of the harmonics in order to obtain time dependence of $E_\theta$ at some angles. Fig. 12 shows comparison of the calculated for $\theta = 60^\circ$ waveform with the results of 3D FDTD solver. An excellent agreement is observed.

More waveforms of $E_\theta$ at $R = 15\,\text{mm}$ for several angles $\theta$ are plotted in Fig. 13.

Typically of interest are the waveforms in the far zone. In order to calculate them we need to perform some transformation from the near zone where we evaluate the fields with FDTD-scheme into the far zone. To this aim let us apply Fourier transform to Equation (13) that yields an ordinary differential equation:

$$\left(\frac{d^2}{dr^2} - \left((q_n/r)^2 - \omega^2\right)\right) E_n(r,\omega) = 0 \tag{40}$$

Equation (40) is supplemented with initial condition $E_n(R,\omega) = E_n^0(\omega)$, where $E_n^0(\omega)$ is the spectrum of the mode amplitude recorded at radius $R$ in the near zone. The solution to this problem that describes

outgoing wave can be written as follows:

$$E_n(r,\omega) = E_n^0(\omega)\sqrt{\frac{r}{R_0}}\frac{H_{b_n}^{(2)}(\omega r)}{H_{b_n}^{(2)}(\omega R_0)} \tag{41}$$

here $H_\nu^{(2)}(\cdot)$ is Hankel function of the second kind, $b_n = \sqrt{1/4 + n(n+1)}$.

Formula (41) allows obtaining spectrum of the radiated field at any distance off the antenna. Using asymptotic of the Hankel function for large argument we obtain the following formula for the mode amplitude spectrum in the far zone:

$$E_n(\omega,r)|_{r\to\infty} = \sqrt{\frac{2}{R_0\pi}}\frac{E_n^0(\omega)}{\sqrt{\omega}H_{b_n}^{(2)}(\omega R_0)}e^{\frac{\pi}{2}i(b_n+1/2)-i\omega r} \tag{42}$$

It should be noted that the $r^{-1}$ decay was factored earlier in (6).

This formula can be used for near-to-far zone transformation of the mode amplitudes. Waveforms of the mode amplitudes are recorded at some radius during FDTD marching in time; then they are transformed into FD by FFT; there formula (42) is applied, and the resulted spectra are turned back to TD by IFFT yielding waveforms in the far zone. Finally the mode amplitudes are summed up in series (6) with mode functions for free space (39) calculated for directions of interest. It allows one to calculate the waveforms of the fields in the far zone for any given direction. Alternatively, if one is interested in calculating a radiation pattern at some frequency then the last IFFT step should be omitted and the mode amplitudes spectral density at the frequency of interest being summed up with the spherical harmonics yield the radiation pattern.

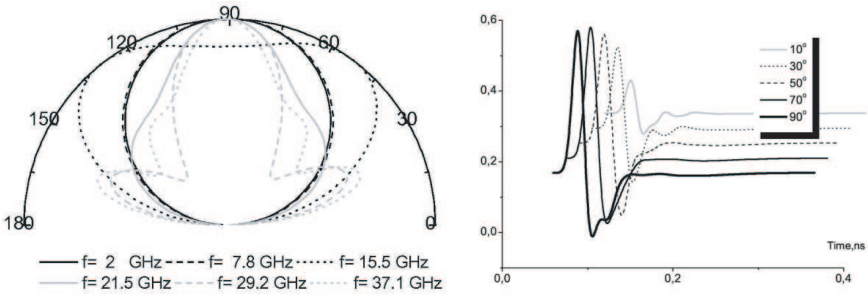


**Figure 14.** Radiation patterns and radiated waveforms in the far zone.

Some examples of calculated radiation patterns at several frequencies and waveforms at several polar angles are plotted in Fig. 14.

## 7. CONCLUSIONS

A new method is proposed for Time Domain analysis of structures consisting of regular waveguide regions with abrupt discontinuities/junctions. It is based on applying the technique of mode matching, which is widely used in the Frequency Domain, to a similar problem considered in the Time Domain.

We considered several numerical examples of applying the proposed method and demonstrated good agreement with reference results.

The method of Mode Matching in Time Domain possesses all the benefits of time domain techniques (obtaining the waveforms and as a result a wideband spectra in one simulation) and allows separate treating of the independent mode channels with 1D FDTD schemes that significantly reduces dimensionality of the problem.

The method was demonstrated to be able to efficiently calculate the pulse radiation of some kind of antennas that can be presented as a finite length regular conical line. Besides the considered bi-conical antenna in this way the following antennas can be considered: TEM-horn, bow-tie antenna, disc-cone antenna, V-antenna, ridge antenna etc.

Further improvement of the proposed method can be done by explicitly accounting edge conditions in the field matching procedure [43, 44] similar to how it is done in Coupled-Integral-Equations Technique [42].

## APPENDIX A.

In this appendix, we are going to derive the update equations for the mode amplitudes at the matching cross-section (28).

To this end we use single sided finite differences (23)–(24) in order to obtain the mode amplitudes for the magnetic fields at the aperture:

$$\begin{aligned}
&\mathbf{v}^{(2)}|_0^{k+1} = \mathbf{v}^{(2)}|_0^{k} - 2\mathbf{S}^{(2)} \cdot \left(\mathbf{i}^{(2)}|_{0.5}^{k+0.5} - \mathbf{i}^{(2)}|_0^{k+0.5}\right) \\
&\quad \Rightarrow \quad \mathbf{i}^{(2)}|_0^{k+0.5} = \mathbf{i}^{(2)}|_{0.5}^{k+0.5} + \tfrac{1}{2}\left(\mathbf{S}^{(2)}\right)^{-1}\left(\mathbf{v}^{(2)}|_0^{k+1} - \mathbf{v}^{(2)}|_0^{k}\right) \\
&\mathbf{v}^{(1)}|_0^{k+1} = \mathbf{v}^{(1)}|_0^{k} - 2\mathbf{S}^{(1)} \cdot \left(\mathbf{i}^{(1)}|_0^{k+0.5} - \mathbf{i}^{(1)}|_{-0.5}^{k+0.5}\right) \\
&\quad \Rightarrow \quad \mathbf{i}^{(1)}|_0^{k+0.5} = \mathbf{i}^{(1)}|_{-0.5}^{k+0.5} - \tfrac{1}{2}\left(\mathbf{S}^{(1)}\right)^{-1}\left(\mathbf{v}^{(1)}|_0^{k+1} - \mathbf{v}^{(1)}|_0^{k}\right)
\end{aligned} \tag{A1}$$

Then we substitute these expressions into the second matrix equation in (26) that represents the condition of magnetic field continuity over the aperture:

$$\mathbf{i}^{(1)}|_{-0.5}^{k+0.5} - \frac{1}{2}\left(\mathbf{S}^{(1)}\right)^{-1}\left(\mathbf{v}^{(1)}|_{0}^{k+1} - \mathbf{v}^{(1)}|_{0}^{k}\right) = \mathbf{M}^{T}\cdot\left(\mathbf{i}^{(2)}|_{0.5}^{k+0.5} + \frac{1}{2}\left(\mathbf{S}^{(2)}\right)^{-1}\left(\mathbf{v}^{(2)}|_{0}^{k+1} - \mathbf{v}^{(2)}|_{0}^{k}\right)\right) \quad \text{(A2)}$$

The first matrix equation from (26) is used in order to exclude $\mathbf{v}^{(2)}$ from the above equation:

$$\mathbf{v}^{(2)}|_{0}^{k} = \mathbf{M}\cdot\mathbf{v}^{(1)}|_{0}^{k} \Rightarrow \left(\mathbf{v}^{(2)}|_{0}^{k+1} - \mathbf{v}^{(2)}|_{0}^{k}\right) = \mathbf{M}\cdot\left(\mathbf{v}^{(1)}|_{0}^{k+1} - \mathbf{v}^{(1)}|_{0}^{k}\right) \quad \text{(A3)}$$

By substituting it into (A2) we arrived to:

$$\mathbf{i}^{(1)}|_{-0.5}^{k+0.5} - \frac{1}{2}\left(\mathbf{S}^{(1)}\right)^{-1}\left(\mathbf{v}^{(1)}|_{0}^{k+1} - \mathbf{v}^{(1)}|_{0}^{k}\right) = \mathbf{M}^{T}\cdot\left(\mathbf{i}^{(2)}|_{0.5}^{k+0.5} + \frac{1}{2}\left(\mathbf{S}^{(2)}\right)^{-1}\mathbf{M}\cdot\left(\mathbf{v}^{(1)}|_{0}^{k+1} - \mathbf{v}^{(1)}|_{0}^{k}\right)\right) \quad \text{(A4)}$$

It can be considered as a linear equation relating the sought increment of electric modal amplitudes $\left(\mathbf{v}^{(1)}|_{0}^{k+1} - \mathbf{v}^{(1)}|_{0}^{k}\right)$ with the known values of magnetic modal amplitudes from the left and right of the junction at time step $k + 0.5$:

$$\frac{1}{2}\left(\left(\mathbf{S}^{(1)}\right)^{-1} + \mathbf{M}^{T}\cdot\left(\mathbf{S}^{(2)}\right)^{-1}\mathbf{M}\right)\left(\mathbf{v}^{(1)}|_{0}^{k+1} - \mathbf{v}^{(1)}|_{0}^{k}\right) = \mathbf{i}^{(1)}|_{-0.5}^{k+0.5} - \mathbf{M}^{T}\cdot\mathbf{i}^{(2)}|_{0.5}^{k+0.5} \quad \text{(A5)}$$

This equation is solved by inverting the nonsingular matrix $\mathbf{F}$ (see (29)) that yields the final updating formula (28) for $\mathbf{v}^{(1)}|_{0}^{k+1}$.

## REFERENCES


1. Rao, S. M., *Time Domain Electromagnetics*, Department of Electrical Engineering, Aubum University, Aubum, AL, 1999.
2. Taflove, A. and S. Hagness, *Computational Eletrodynamics: The Finite-Difference Time-Domain Method*, 2nd edition, Artech House, 2000.
3. Pozar, D. M., *Microwave Engineering*, 2nd Edition, University of Massachusetts at Amherst, 1998.
4. Marcuvitz, N., *Waveguide Handbook*, Peter Peregrinus Ltd, 1993.

5. Mittra, R. and S. Lee, *Analytical Techniques in the Theory of Guided Waves*, University of Illinois, New York, 1971.
6. Kisunko, G. V., *Electrodynamics of Hollow Systems*, VKAS, Leningrad, USSR, 1949 (in Russian).
7. Borisov, V. V., "Electromagnetic field of a current with arbitrary time dependence distributed on the surface of a sphere," *Radiophysics and Quantum Electronics*, Vol. 19, No. 12, 1291–1298, 1976.
8. Borisov, V. V., "Nonperiodic electromagnetic fields in a sectoral horn," *Radiotekhnika and Elektronika*, Vol. 28, 450–460, Mar. 1983 (in Russian).
9. Borisov, V. V., "Excitation of nonperiodic fields in a conical horn," *Radiotekhnika and Elektronika*, Vol. 30, 443–447, Mar. 1985 (in Russian).
10. Borisov, V. V., *Transients in Waveguides*, Publishing House of Leningrad State University, Leningrad, 1991 (in Russian).
11. Tretyakov, O. A., "Mode basis method," *Radiotekhnika and Elektronika*, Vol. 31, No. 6, 1071–1082, 1986 (in Russian).
12. Tretyakov, O. A., "Evolutionary equations for the theory of waveguides," *IEEE Antennas and Propagation Society, AP-S International Symposium (Digest)*, Vol. 3, 1973–1976, 1994.
13. Tretyakov, O. A., "Evolutionary waveguide equations," *Radiotekhnika and Elektronika*, Vol. 34, No. 5, 917–926, 1989.
14. Tretyakov, O. A., "Essentials of nonstationary and nonlinear electromagnetic field theory," chapter in Hashimoto M., Idemen M., Tretyakov O. A., *Analytical and Numerical Methods in Electromagnetic Wave Theory*, 572, Tokyo, Science House Co, Ltd, 1993.
15. Nikitskiy, S. B., O. A. Tretyakov, and K. M. Yemelyanov, "Electromagnetic step signal propagation in lossy waveguide," *Telecommunications and Radio Engineering*, Vol. 51, No. 2, 149–159, 1997.
16. Kristensson, G., "Transient electromagnetic wave propagation in waveguides," *Journal of Electromagnetic Waves and Applications*, Vol. 9, 645–671, 1995.
17. Geyi, W., "A time-domain theory of waveguide," *Progress In Electromagnetics Research*, Vol. 59, 267–297, 2006.
18. Tretyakov, O. A. and S. V. Chumachenko, "Oscillations in a resonator filled with a time-varying dielectric medium," *Telecommunications and Radio Engineering*, Vol. 52, No. 6, 36–45, 1998.
19. Butrym, A. Y., Y. Zheng, and O. A. Tretyakov, "Transient

diffraction on a permittivity step in a waveguide: Closed-form solution in time domain," *Journal of Electromagnetic Waves and Applications*, Vol. 18, No. 7, 861–876, 2004.

20. Butrym, A. Y. and M. N. Legenkiy, "Charge transport by a pulse E-wave in a waveguide with conductive medium," *Progress In Electromagnetics Research B*, Vol. 15, 325–346, 2009.
21. Butrym, A. Y. and B. A. Kochetov, "Mode basis method for spherical TEM-transmission lines and antennas," *Proc. International Conference on Antenna Theory and Techniques*, 243–245, (ICATT-07), Sevastopol, 2007.
22. Aksoy, S. and O. A. Tretyakov, "Study of a time variant cavity system," *Journal of Electromagnetic Waves and Applications*, Vol. 16, No. 11, 1535–1553, 2002.
23. Tretyakov, O. A. and F. Erden, "Temporal cavity oscillations caused by a wide-band waveform," *Progress In Electromagnetics Research B*, Vol. 6, 183–204, 2008.
24. Geyi, W., "Time-domain theory of metal cavity resonator," *Progress In Electromagnetics Research*, Vol. 78, 219–253, 2008.
25. Antyufeyeva, M. S., A. Y. Butrym, and O. A. Tretyakov, "Transient electromagnetic fields in cavity with dispersive double negative medium," *Progress In Electromagnetics Research M*, Vol. 8, 51–65, 2009.
26. Aksoy, S. and O. A. Tretyakov, "Evolution equations for analytical study of digital signals in waveguides," *Journal of Electromagnetic Waves and Applications*, Vol. 17, No. 12, 263–270, 2004.
27. Butrym, A. Y. and B. A. Kochetov, "Time domain mode basis method for a waveguide with transverse inhomogeneous multi-connected cross-section. 1. The general theory of method," *Radio Physics and Radio Astronomy*, Vol. 14, No. 2, 162–173, 2009 (in Russian).
28. Butrym, A. Y. and B. A. Kochetov, "Time domain mode basis method for a waveguide with transverse inhomogeneous multi-connected cross-section. 2. Example of numerical implementation of the method," *Radio Physics and Radio Astronomy*, Vol. 14, No. 3, 266–277, 2009 (in Russian).
29. Dumin, A. N., "Radiation of transient localized waves from an open-ended coaxial waveguide with infinite flange," *Telecommunications and Radio Engineering*, Vol. 53, No. 6, 30–34, 1999.
30. Tretyakov, O. A. and A. N. Dumin, "Emission of nonstationary electromagnetic fields by a plane radiator," *Telecommunications and Radio Engineering*, Vol. 54, No. 1, 2–15, 2000.

31. Shlivinski, A. and E. Heyman, "Time-domain near-field analysis of short-pulse antennas. Part I: Spherical wave (multipole) expansion," *IEEE Trans. Antennas Propag.*, Vol. 47, No. 2, 271–279, Feb. 1999.
32. Tretyakov, O., A. Dumin, O. Dumina, and V. Katrich, "Modal basis method in radiation problems," *Proc. Int. Conf. on Math. Methods in Electromagnetic Theory (MMET-2004)*, 312–314, Dnepropetrovsk, Ukraine, 2004.
33. Dumin, O. M., O. O. Dumina, and V. O. Katrich, "Propagation of spherical transient electromagnetic wave through radially inhomogeneous medium," *Proc. Int. Conf. on Ultrawideband and Ultrashort Impulse Signals (UWBUSIS-2006)*, 276–278, Sevastopol, Ukraine, Sep. 18–22, 2006.
34. Butrym, A. Y. and B. A. Kochetov, "Mode expansion in time domain for conical lines with angular medium inhomogeneity," *Progress In Electromagnetics Research B*, Vol. 19, 151–176, 2010.
35. Zheng, Y., B. A. Kochetov, and A. Y. Butrym, "Finite difference scheme in time domain and analytical solution for Klein-Gordon equation," *Bulletin of Karazin Kharkiv National University,* No. 712, "Radiophysics and Electronics," No. 10, 91–94, 2006 (in Russian).
36. Butrym, A. Y. and M. N. Legenkiy, "Comparison of absorbing boundary conditions for numerical analysis of periodic structures," *Proc. of International Conference on Antenna Theory and Techniques*, 239–242, Sevastopol, Ukraine, Sep. 17–21, 2007.
37. Uher, J., J. Bornemann, and U. Rosenberg, *Waveguide Components for Antenna Feed Systems: Theory and CAD*, Artech House, Boston, 1993.
38. Kirilenko, A. A., V. I. Tkachenko, L. A. Rud, and D. Y. Kulik, "The mode-matching technique and fast numerical models of arbitrary coordinate waveguide objects," *Quasi-optical Control of Intense Microwave Transmission*, J. L. Hirshfield and M. I. Petelin (eds.), 41–53, Springer, Netherlands, 2005.
39. Kirilenko, A. A., D. Y. Kulik, and V. I. Tkachenko, "General scheme of the mode-matching technique as a basis for generalized solutions to the internal boundary-value problems," *Telecommunications and Radio Engeneering*, Vol. 60, No. 12, 159–170, 2003.
40. Legenkiy, M., Y. Zheng, and A. Butrym, "Mode matching in time domain," *Proceedings of UWBUSIS*, 225–227, Sevastopol, Ukraine, Sep. 15–19, 2008.
41. Butrym, A., B. Kochetov, and M. Legenkiy, "Numerical analysis of simple TEM conical-like antennas using mode matching in time

domain," *Proceedings of EuCAP 2009*, 3471–3475, Berlin, 2009.

42. Bornemann, J., "On the acceleration of the coupled-integral-equations technique and its application to multistub E-plane discontinuities," *Journal of Electromagnetic Waves and Applications*, Vol. 13, 539–554, 1999.
43. Amari, S., A. Motamedi, J. Bornemann, and R. Vahldieck, "Global edge-conditioned basis functions from local solutions of Maxwell's equations," *IEEE MTT-S International Microwave Symposium Digest*, 1373–1376, Denver, USA, 1997.
44. Damaschke, J. M., S. Amari, and J. Bornemann, "Fast and accurate mode-spectrum analysis of waveguide structures using a new set of edge-conditioned basis functions," *International Journal of RF and Microwave Computer-aided Engineering*, Vol. 8, No. 3, 215–225, 1998.
45. Luo, S. and Z. Chen, "An efficient modal FDTD for absorbing boundary conditions and incident wave generator in waveguide structures," *Progress In Electromagnetic Research*, Vol. 68, 229–246, 2007.
46. Sirenko, Y. K., "Exact 'absorbing' conditions in outer initial boundary-value problems of electrodynamics of nonsinusoidal waves. Part 3. Compact inhomogeneities in free space," *Telecommunications and Radio Engineering*, Vol. 57, No. 12, 1–31, 2002.
47. Lo, Y. T. and S. W. Lee, *Antenna Handbook. Volume 1 Fundamentals and Mathematical Techniques*, Chapman & Hall, New York, 1993.
48. Gustafsson, B., H.-O. Kreiss, and J. Oliger, *Time-dependent Problems and Difference Methods*, Willey-Interscience, New York, 1995.
49. Samaddar, S. N. and E. L. Mokole, "Biconical antennas with unequal cone angles," *IEEE Trans. Antennas Propagat.*, Vol. 46, 181–193, Feb. 1998.